A Hybrid Landmark and Contour-Matching Image Registration Model

Mia Mojica — Ontario Tech University, Oshawa, ON, Canada
Mehran Ebrahimi — Ontario Tech University, Oshawa, ON, Canada
Email: {Mia.Mojica, Mehran.Ebrahimi}@OntarioTechU.ca

Abstract

In this manuscript, we propose a novel hybrid Landmark and Contour-Matching (LCM) image registration model to align image pairs. The proposed model uses image contour information to supplement missing edge information in between exact landmarks. We demonstrate that the model circumvents the drawbacks associated with a straightforward application of the Thin Plate Spline (TPS) registration technique.

The proposed model provides higher post-registration Dice similarity between the reference and registered template images by improving the image overlap away from major landmarks and visually reduces the appearance of the "unnatural bending" typically present in TPS-registered images. We also show that naively increasing the number of landmarks in a TPS model does not always guarantee an accurate registration result. We indicate how the proposed model using even less number of exact landmarks along with additional approximate contour information provided suitable results, as opposed to the TPS model. Lastly, the proposed model produces physically relevant registration results with improved Dice similarity indices even when landmark localization errors are present in data.

Overall, the proposed Landmark and Contour-Matching (LCM) model increases the flexibility of the TPS approach especially when only a few landmarks can be defined, when defining too many landmarks leads to high oscillations in the registration transformations, or when the identification of exact landmarks is susceptible to human error.

1 Introduction

Thin plate spline (TPS) data interpolation and approximation are a spline-based technique that has been applied successfully in various fields such as medical imaging, oceanography, geosciences, and shape analysis in general [1–8].

As a landmark-based registration technique, the use of TPS transformations to describe a non-rigid deformation results to a system of equations that have a closed-form solution [5]. In addition, it produces physically relevant smooth transformations.

While the implementation of a TPS approach is convenient and straightforward, the method comes with some drawbacks. Similar to other landmark-based registration methods, image similarity tends to suffer away from landmarks [9]. Visually, this could result to abnormalities (e.g., unnatural bending, incorrect scaling of image features) in the registered image (see Figure 1c).

Naturally, one could consider increasing the number of landmark correspondences in order to improve image overlap between the reference and registered template. Thin plate splines, however, are radial basis functions that have global support. This means that sample points act both as knots and interpolating points, which could then result to a number of computational issues. First, increasing the number of landmarks would involve the inversion of a TPS kernel matrix – an operation of order $\mathcal{O}(K^3)$, where K is the number of landmark pairs. Increasing the number of landmarks also leads to an increase in the condition number of the TPS kernel matrix that could likewise translate to deformities in the registered image as in Figures 1d-1f.

Figure 1d is the result of solving a TPS system with 58 interpolation conditions. Meanwhile, the TPS-registered images in Figures 1e and 1f suffer from stretching artefacts. More specifically, the metacarpophalangeal joints at the base of the middle finger in both images appear stretched significantly more than the original template image. The joint at the base of the ring finger in Figure 1e also appears curved even when the external finger contour is straight.

Ill-conditioning also occurs in the presence of data points that are too close together [10]. In such a case, exact interpolation is sensible only if the intensity values at the two close data sites are themselves close [11].

In this paper, we aim to address these issues associated with TPS registration. We will introduce a registration model that pairs with the landmark detection method we proposed in [12]. The model only requires a small number of feature points as centers of the TPS radial basis functions. It also incorporates approximate contour information to increase registration accuracy and avoid the visual deformities commonly induced by a purely TPS-based approach in the transformed template.

Lastly, since landmark selection in medical images is typically done manually and is thus susceptible to errors, it is important for a registration model to cater to such localization errors. We will demonstrate that the model outperforms the TPS approach in such cases.

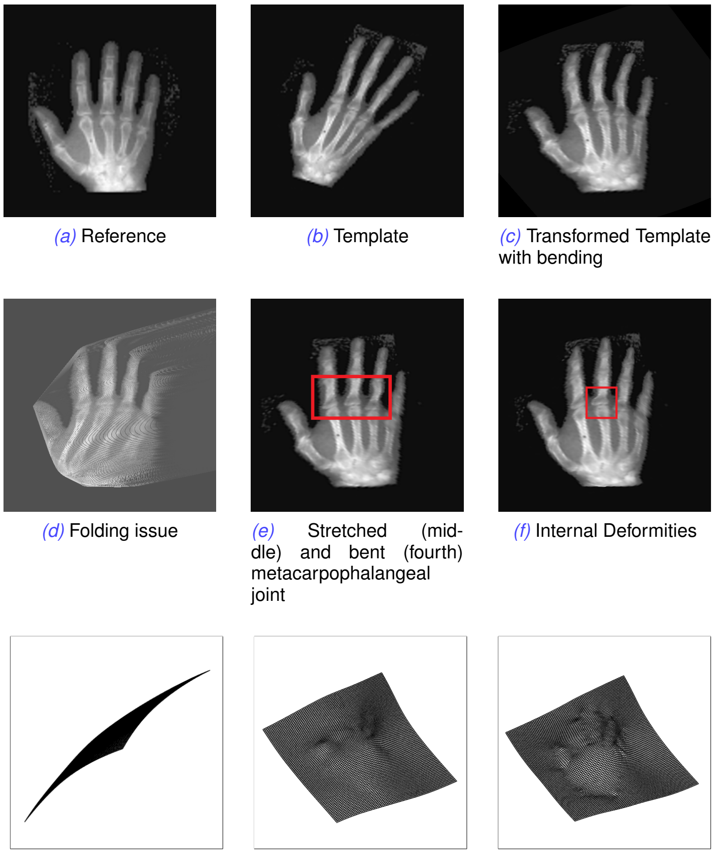

(a) Reference (b) Template (c) Transformed Template with bending
(d) Folding issue (e) Stretched (middle) and bent (fourth) metacarpophalangeal joint (f) Internal Deformities
(g) Sample TPS Transf. 1 (h) Sample TPS Transf. 2 (i) Sample TPS Transf. 3

Fig. 1: Drawbacks of thin plate spline registration in medical imaging. (a) Reference, (b) template, (c) unnatural bending in registered image, (d) folding issue in ill-conditioned TPS systems, (e)-(f) deformities induced by the TPS transformations with too many knots, (g)-(i) TPS transformations associated with the registered images in (d)-(f).

2 Proposed Landmark and Contour-Matching Model

Let $\mathcal{R}$ and $\mathcal{T}$ be the reference and template images with exact (major) landmarks $\{r_j\}_{j=1}^{K}$ and $\{t_j\}_{j=1}^{K}$, respectively. Also, let $\left\{\overset{*}{r}_i\right\}_{i=1}^{L}$ and $\left\{\overset{*}{t}_i\right\}_{i=1}^{L}$ be an ordered set of sampling points that trace the contours of an object of interest present in $\mathcal{R}$ and $\mathcal{T}$. We aim to solve the optimization problem of

$$\theta^* = \min_{\theta} \mathcal{D}^{\mathsf{LM}}[\theta] + \alpha \mathcal{C}[\theta] \tag{1}$$

in which θ is a thin plate spline transformation.

For a 2-dimensional registration problem, the optimal solution of (1) has the form $\theta^* = [\theta^1, \theta^2]^T$, where

$$\theta^i(x) = \sum_{j=1}^{K} c_j^i \left\|x-t_j\right\|^2 \log\left\|x-t_j\right\| + w_0^i + w_1^i x^1 + w_2^i x^2 \qquad (2)$$

and $c_j^i, w_l^i \in \mathbb{R}$ for $i=1,2,\ j=1,\dots,K,\ l=0,1,2$, and $x=[x^1,x^2]^T$. In (1),

- $\mathcal{D}^{\mathsf{LM}}$ denotes sum of squared landmark distances

$$\mathcal{D}^{\mathsf{LM}}[\theta] = \sum_{j=1}^{K} \left\|\theta(t_j)-r_j\right\|^2,$$

- $\mathcal{C}$ denotes the contour matching term

$$\mathcal{C}[\theta] = \sum_{i=1}^{L} \frac{1}{2}\left[1-\left(v\left[\theta\left(\overset{*}{t}_i\right)\right]\cdot v\left[\overset{*}{r}_i\right]\right)^2\right], \qquad (3)$$

  and

- $v\left[\theta\left(\overset{*}{t}_i\right)\right]\cdot v\left[\overset{*}{r}_i\right]$ denotes the cosine of the angle between corresponding unit vectors $v\left[\theta\left(\overset{*}{\mathbf{t}}_i\right)\right]$ and $v\left[\overset{*}{\mathbf{r}}_i\right]$ formed by consecutive contour-approximating points in the transformed template and reference images, respectively.

The components of the contour matching term are given by

- $$v\left[\overset{*}{r}_i\right] = \frac{\overrightarrow{\overset{*}{r}_i\overset{*}{r}_{i+1}}}{\left\|\overrightarrow{\overset{*}{r}_i\overset{*}{r}_{i+1}}\right\|} = \frac{\left\langle \overset{*}{r}{}^1_{i+1}-\overset{*}{r}{}^1_i, \overset{*}{r}{}^2_{i+1}-\overset{*}{r}{}^2_i\right\rangle}{\left\|\left\langle \overset{*}{r}{}^1_{i+1}-\overset{*}{r}{}^1_i, \overset{*}{r}{}^2_{i+1}-\overset{*}{r}{}^2_i\right\rangle\right\|}$$

  and

- $$v\left[\theta\left(\overset{*}{t}_i\right)\right] = \frac{\overrightarrow{\theta\left(\overset{*}{t}_i\right)\theta\left(\overset{*}{t}_{i+1}\right)}}{\left\|\overrightarrow{\theta\left(\overset{*}{t}_i\right)\theta\left(\overset{*}{t}_{i+1}\right)}\right\|} = \frac{\left\langle \theta^1\left(\overset{*}{t}_{i+1}\right)-\theta^1\left(\overset{*}{t}_i\right), \theta^2\left(\overset{*}{t}_{i+1}\right)-\theta^2\left(\overset{*}{t}_i\right)\right\rangle}{\left\|\left\langle \theta^1\left(\overset{*}{t}_{i+1}\right)-\theta^1\left(\overset{*}{t}_i\right), \theta^2\left(\overset{*}{t}_{i+1}\right)-\theta^2\left(\overset{*}{t}_i\right)\right\rangle\right\|}.$$

Minimizing the contour-matching term $\mathcal{C}$ is equivalent to maximizing the dot product of corresponding vectors that approximate the edges in the pair of images being registered or maximizing the similarity in the orientation of these unit vectors without any constraints on scaling. Therefore, the registration problem in (1) relaxes the TPS interpolation condition

$$\mathcal{D}^{\mathsf{LM}}[\theta] = 0$$

and balances the overlap of the exact landmarks and the similarity between the orientation of the image contours.

An example of the setup required in the proposed Landmark and Contour-Matching (LCM) model is shown in Figure 2.

3 Experiments

2D hand images from [5] were used to validate the proposed Landmark and Contour Matching model.

Major reference-template landmark and contour-approximating point pairings were defined prior to registration. In our experiments, the major landmarks (i.e., the fingertips and the cusps in between adjacent fingers) were identified via the interest point detection method presented in [12]. Meanwhile, the contour-approximating points

$$\left\{\overset{*}{r}_i\right\}_{i=1}^{L} \text{ and } \left\{\overset{*}{t}_i\right\}_{i=1}^{L}$$

represent an ordered sampling of the connected set of pixels that trace the edges of the hands. We note here that the major landmarks could be selected manually or through a different interest point detection method. Thus, the set of major landmarks need not be a proper subset of the collection of contour-approximating landmarks.

We then solved the constrained optimization problem in (1) using Newton's method to obtain the optimal TPS parameters. At every iteration, the distances between the transformed major template landmarks and their target locations were calculated. In addition, the vectors connecting adjacent contour-approximating landmarks were normalized, and the cosine of the interior angles formed by corresponding unit vector pairs in the reference and transformed template were calculated to measure the overall similarity in orientation of the contours present between the two images.

The exact Hessian of both the landmark and contour-matching terms in (1) were used in the implementation of the Newton method.

In the first set of experiments, we simply performed the steps described above and compared the results of the proposed model against registered images obtained by blindly performing TPS registration (i.e., by solving (1) where $\alpha = 0$) with

1a. only 11 POIs as exact landmarks (Figure 3a)
1b. the 11 POIs in Experiment 1a and a specified number of additional contour-approximating landmarks, all treated as major landmarks (Figure 3b).

The goal of this set of experiments is to determine whether the proposed LCM model indeed addresses the drawbacks of TPS registration. First, we want to observe whether using the same number of exact landmarks as in Experiment 1a but adding extra contour information (from the approximate landmarks) to be used only in the second term $C[\theta]$ lessens the occurrence of unnatural bending and consequently improves the image overlap away from the exact landmarks.

Next, we wish to gauge whether LCM-registered results using few exact landmarks and approximate contour information improves on the results of Experiment 1b, where contour-approximating landmarks are treated as hard interpolation constraints.

The second set of experiments (Experiments 2a and 2b, Figures 4a-4c) is the same as the first, except that a landmark localization error was introduced to one of the major template landmarks. The purpose of these experiments is to determine the accuracy of the registration methods in the presence of landmark localization error. The TRE and Dice coefficients of the registered images resulting from the blind application of TPS are compared against those of the LCM-registered images.

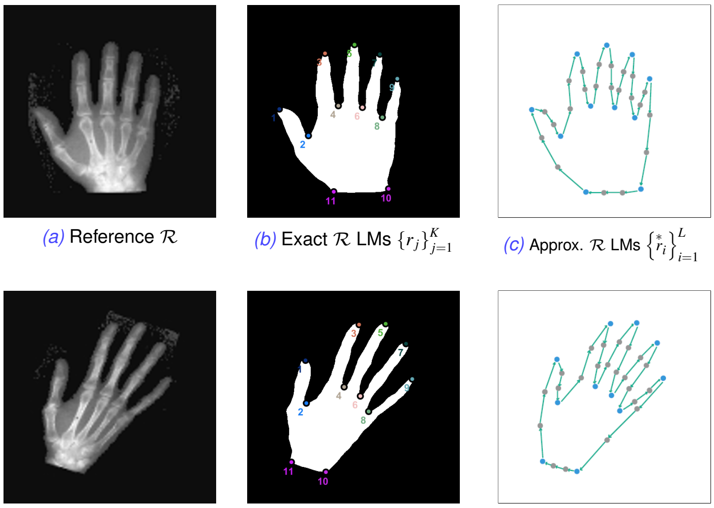

(a) Reference $\mathcal{R}$ *(b)* Exact $\mathcal{R}$ LMs $\{r_j\}_{j=1}^K$ *(c)* Approx. $\mathcal{R}$ LMs $\{\overset{*}{r}_i\}_{i=1}^L$

(d) Template $\mathcal{T}$ *(e)* Exact $\mathcal{T}$ LMs $\{t_j\}_{j=1}^K$ *(f)* Approx. $\mathcal{T}$ LMs $\{\overset{*}{t}_i\}_{i=1}^L$

Fig. 2: Landmark and Contour-Matching (LCM) Model requisites. (a) Reference image, (b) exact/major reference landmarks, (c) exact reference landmarks, contour-approximating points and vectors, (d) template image, (e) exact/major template landmarks, (f) exact template landmarks, contour-approximating points and vectors. Here, number of exact landmarks is $K = 11$ and number of contour-approximating points is $L = 33$.

4 Results

The results of the first set of experiments is displayed in Figure 3a. Observe that imposing only a few hard constraints in the TPS approach yielded registered images where the fingers are slightly bent. The number of exact landmarks used in Experiment 1a is $K = 11$.

Next, for Experiment 1b (Figure 3b) we used 58 contour-approximating landmarks as exact landmarks (i.e., as hard constraints) in the TPS interpolation problem to determine whether an increase in the number of exact landmark correspondences also results to an improvement in the registration accuracy. While the Dice similarity coefficient did increase, the registered image still exhibits some irregularities. For instance, the edge of the fingers, especially those of the middle and ring fingers, appear to have small ridges instead of a smooth edge. Notice that the metacarpophalangeal joints of the middle and ring fingers were also distorted by the registration transformation.

In contrast, LCM-registered templates yielded both improved Dice similarity coefficients compared to Experiment 1a, and visually accurate results (Figures 3c,3d). More specifically, there were no apparent deformities such as bent fingers, bumpy edges, and distorted bones in the LCM results unlike those yielded by Experiments 1a and 1b.

When analyzing the results of Experiments 2a and 2b (with landmark localization error), it is important to note that TPS registration at its core is just an interpolation technique. Therefore, blindly applying the technique naturally results to misregistrations (Figures 4a-4c) – regardless of the number of interpolating points.

The proposed LCM method once again outperformed the TPS approach and resulted to better post-registration Dice image similarities, smaller target registration errors (TRE), and registered images without any abnormalities even in the presence of a landmark error (Figures 4d,4e).

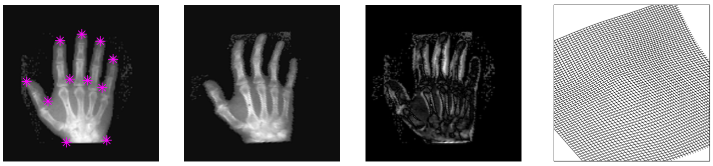

(a) Experiment 1a: TPS using major LMs only ($K = 11$); Post-TPS registration Dice $= 0.82$

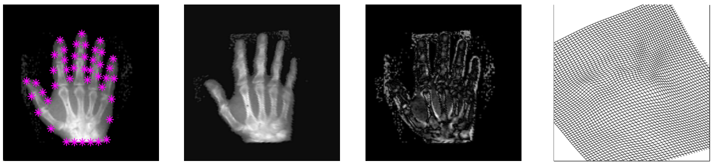

(b) Experiment 1b: TPS using major and contour-approximating LMs as exact LMs ($K = 59$); Post-TPS Registration Dice $= 0.85$

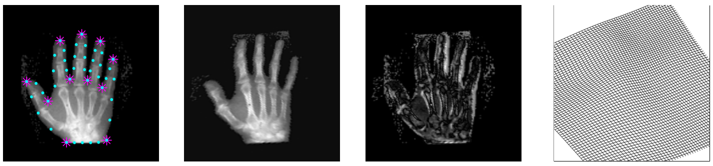

(c) Proposed Method: LCM model using $K = 11$ Major ($*$) and $L = 59$ Contour-approximating ($\cdot$) LMs ; Post-LCM Registration Dice =0.84

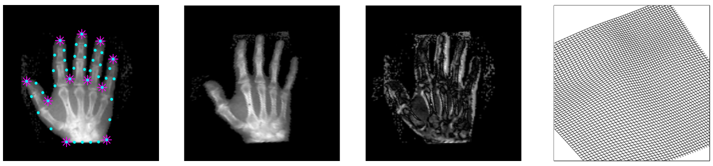

(d) Proposed Method: LCM model using $K = 11$ Major ($*$) and $L = 43$ Contour-approximating ($\cdot$) LMs ; Post-LCM Registration Dice =0.84

Fig. 3: Comparison of TPS and LCM Registration Accuracy. (a) Results of Experiments 1a, (b) results of Experiment 1b. (c)-(d) LCM registration results. Pre-Registration Dice =0.64. (First col) Reference image with exact and contour-approximating landmarks, (Second col) registered image, (Third col) post-registration subtraction image $|R - T[\theta]|$, (Fourth col) optimal transformation. Bending, ridges along the finger contours, and bone deformities are present in the TPS-registered images in (a) and (b). Notably, the LCM-registered images in (c) and (d) do not suffer from such deformities.

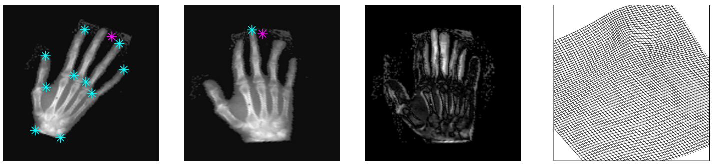

(a) Experiment 2a: TPS using major LMs only ($K = 11$). Localization error was introduced to t_5 (the middle fingertip); Post-TPS registration Dice $= 0.81$; TRE=9.28mm

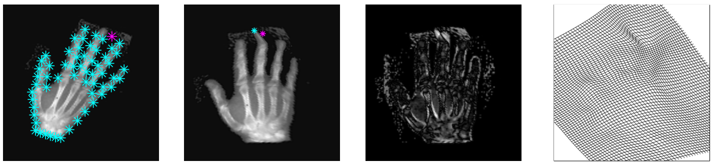

(b) Experiment 2b: TPS using major and contour-approximating LMs as exact LMs ($K = 59$). Localization error was introduced to t_5 (the middle fingertip); Post-TPS registration Dice =0.84; TRE=7.35mm

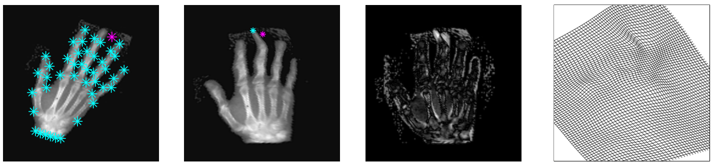

(c) Experiment 2b: TPS using major and contour-approximating LMs as exact LMs ($K = 43$). Localization error was introduced to t_5 (the middle fingertip); Post-TPS registration Dice =0.84; TRE=8.59mm

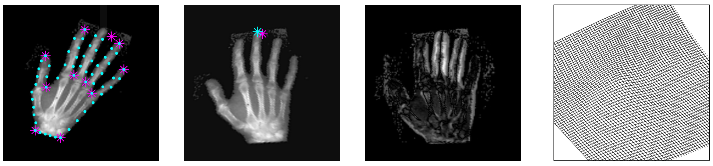

(d) Proposed Method: LCM model using $k = 11$ Major ($*$) and $L = 58$ Contour-approximating ($\cdot$) LMs. Localization error was introduced to t_5 (the middle fingertip); Post-LCM registration Dice =0.81; TRE=4.40mm

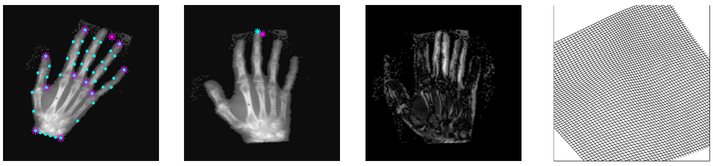

(e) Proposed Method: LCM model using $k = 11$ Major ($*$) and $L = 42$ Contour-approximating ($\cdot$) LMs. Localization error was introduced to t_5 (the middle fingertip); Post-LCM registration Dice =0.82; TRE=4.72mm

Fig. 4: Comparison of TPS and LCM Registration Accuracy for the case when a LM localization error is present in one of the exact LMs (the fifth fingertip). (a) Results of Experiments 2a, (b)-(c) results of Experiment 2b, (d)-(e) LCM registration results. Pre-Registration Dice =0.64. (1st col) Reference image with exact and contour-approximating landmarks, (2nd col) registered image, (3rd col) post-registration subtraction image $|R - T[\theta]|$, (4th col) optimal transformation. Direct application of hard LM interpolation conditions when 1 LM localization error was present in the data resulted to misregistrations and seemingly bent or distorted fingers like in (a)-(c). LCM provides good image overlaps and mitigates the effect of the LM error, as in (d)-(e).

5 Conclusions

In this paper, we proposed a new registration model that uses contour-approximating landmarks to supplement missing edge information in between defined landmarks. We demonstrated that the model was able to circumvent drawbacks associated with the straightforward application of the TPS registration technique.

The LCM model was shown to increase the post-registration Dice similarity between the reference and registered template by improving the image overlap away from major landmarks. Consequently, this reduced the appearance of the unnatural bending in image regions bordered by the data interpolation points (major landmark locations).

We also showed that naively increasing the number of interpolation conditions does not always guarantee a clinically accurate registration result. Doing so resulted to an ill-conditioned problem, made the TPS technique computationally more expensive, and also caused visual deformities in the transformed template. As with addressing the first TPS issue, we showed that solving the LCM registration problem with less exact landmarks and additional approximate contour information provided accurate results.

The LCM model also produced physically accurate registration results with improved Dice similarity indices even when landmark localization errors were present in the data.

Overall, the LCM model increases the flexibility of the TPS approach especially when only a few repeatable landmarks can be defined, when defining too many landmarks leads to high oscillations in the registration transformations, or when the identification of exact landmarks is susceptible to human error.

Acknowledgments

This work was supported in part by an NSERC Discovery Development Grant for Mehran Ebrahimi. Mia Mojica was supported by a Doctoral Ontario Trillium Scholarship (OTS).

References

[1] D. S. Trossman, L. Thompson, and S. L. Hautala, "Application of thin-plate splines in two dimensions to oceanographic tracer data," *Journal of Atmospheric and Oceanic Technology*, vol. 28, no. 11, pp. 1522–1538, 2011.

[2] M. Lepot, J.-B. Aubin, and F. H. Clemens, "Interpolation in time series: An introductive overview of existing methods, their performance criteria and uncertainty assessment," *Water*, vol. 9, no. 10, p. 796, 2017.

[3] G. Donato and S. Belongie, "Approximate thin plate spline mappings," in *European conference on computer vision*. Springer, 2002, pp. 21–31.

[4] G. E. Christensen and H. J. Johnson, "Consistent image registration," *IEEE transactions on medical imaging*, vol. 20, no. 7, pp. 568–582, 2001.

[5] J. Modersitzki, *FAIR: flexible algorithms for image registration*. SIAM, 2009, vol. 6.

[6] G. Ahmadian, S. Bohun, and M. Ebrahimi, "Evaluation of a coherent point drift algorithm for breast image registration via surface markers," *Journal of Computational Vision and Imaging Systems*, vol. 2, Open Access, October 2016.

[7] P. Siegler, M. Ebrahimi, C. Holloway, G. Thevathasan, D. B. Plewes, and A. L. Martel, "Supine breast MRI and assessment of future clinical applications," *European Journal of Radiology*, vol. 81, no. S1, pp. 153–155, 2012.

[8] M. Ebrahimi, P. Siegler, C. H. A. Modhafar, D. B. Plewes, and A. L. Martel, "Using surface markers for MRI guided breast conserving surgery: A feasibility survey," *Physics in Medicine and Biology*, no. 59, pp. 1589–1605, 2014.

[9] B. Fischer and J. Modersitzki, "Combining landmark and intensity driven registrations," in *PAMM: Proceedings in Applied Mathematics and Mechanics*, vol. 3, no. 1. Wiley Online Library, 2003, pp. 32–35.

[10] T. O. Ramsay, "A bivariate finite element smoothing spline applied to image registration." 2001.

[11] R. Sibson and G. Stone, "Computation of thin-plate splines," *SIAM Journal on Scientific and Statistical Computing*, vol. 12, no. 6, pp. 1304–1313, 1991.

[12] M. Mojica, M. Pop, and M. Ebrahimi, *Automatic Detection of Landmarks for Fast Cardiac MR Image Registration*. Manuscript submitted for publication., 2020.